NAVAL POSTGRADUATE SCHOOL
Monterey, California

THESIS

EXPERIMENTAL INVESTIGATION OF SINKING A BUOYANT BODY IN WATER WITH BUBBLES

by

Leonard B. Pringle

June 2000

Thesis Advisor: Bruce Denardo
Co-Advisor: Ashok Gopinath

Approved for public release; distribution is unlimited

REPORT DOCUMENTATION PAGE

Form Approved OMB No. 0704-0188

1. AGENCY USE ONLY	2. REPORT DATE	3. REPORT TYPE AND DATES COVERED
	June 2000	Master's Thesis

4. TITLE AND SUBTITLE
Experimental Investigation of Sinking a Buoyant Body in Water with Bubbles

5. FUNDING NUMBERS

6. AUTHOR(S)
Pringle, Leonard B.

7. PERFORMING ORGANIZATION NAME(S) AND ADDRESS(ES)
Naval Postgraduate School
Monterey CA 93943-5000

8. PERFORMING ORGANIZATION REPORT NUMBER

9. SPONSORING/MONITORING AGENCY NAME(S) AND ADDRESS(ES)

10. SPONSORING/MONITORING AGENCY REPORT NUMBER

11. SUPPLEMENTARY NOTES
The views expressed in this thesis are those of the authors and do not reflect the official policy or position of the Department of Defense or the U.S. Government.

12a. DISTRIBUTION/AVAILABILITY STATEMENT
Approved for public release; distribution is unlimited.

12b. DISTRIBUTION CODE

13. ABSTRACT *(maximum 200 words)*

The introduction of gas bubbles into a liquid decreases the average density, and thus decreases the buoyant force on a floating body. This thesis investigates the critical average density required to sink a buoyant body in water with rising bubbles. A volume of bubbly water is created in a clear acrylic tube of inner diameter 30 cm and height 60 cm, that is closed at the bottom and open at the top. An array of diffusers at the bottom produces 2 mm diameter bubbles distributed uniformly over the cross section of the tube. A 10-cm diameter hollow steel ball whose average density is varied from 0.70 to 0.99 g/cm^3 is employed as the buoyant body. A theory of the critical density for sinking is developed, and predicts that the average fluid density is greater than the ball density for sinking. The experimental data, which include a quantitative error analysis, agree well with the theory for average ball densities from 0.94 to 0.99 g/cm^3, but show a definite trend of fluid densities that are smaller than those predicted for 0.70 to 0.94 g/cm^3.

14. SUBJECT TERMS: Water, Density, Specific Gravity, Volume Fraction, Bubbles, Buoyancy, Non-Newtonian Fluid

15. NUMBER OF PAGES 58

16. PRICE CODE

17. SECURITY CLASSIFICATION OF REPORT	18. SECURITY CLASSIFICATION OF THIS PAGE	19. SECURITY CLASSIFICATION OF ABSTRACT	20. LIMITATION OF ABSTRACT
Unclassified	Unclassified	Unclassified	UL

NSN 7540-01-280-5500

Standard Form 298 (Rev. 2-89)
Prescribed by ANSI Std. 239-18 298-102

Approved for public release; distribution is unlimited.

EXPERIMENTAL INVESTIGATION OF SINKING A BUOYANT BODY IN WATER WITH BUBBLES

Leonard B. Pringle
Lieutenant Commander, Canadian Forces
B.E., Royal Military College of Canada, 1991

Submitted in partial fulfillment of the
requirements for the degree of

**MASTER OF SCIENCE IN
APPLIED PHYSICS**

from the

**NAVAL POSTGRADUATE SCHOOL
June 2000**

Author: _____
Leonard B. Pringle

Approved by: _____
Bruce Denardo, Thesis Advisor

_____
Ashok Gopinath, Co-Advisor

_____
William B. Maier, Chairman
Department of Physics

ABSTRACT

The introduction of gas bubbles into a liquid decreases the average density, and thus decreases the buoyant force on a floating body. This thesis investigates the critical average density required to sink a buoyant body in water with rising bubbles. A volume of bubbly water is created in a clear acrylic tube of inner diameter 30 cm and height 60 cm, that is closed at the bottom and open at the top. An array of diffusers at the bottom produces 2 mm diameter bubbles distributed uniformly over the cross section of the tube. A 10-cm diameter hollow steel ball whose average density is varied from 0.70 to 0.99 g/cm^3 is employed as the buoyant body. A theory of the critical density for sinking is developed, and predicts that the average fluid density is greater than the ball density for sinking. The experimental data, which include a quantitative error analysis, agree well with the theory for average ball densities from 0.94 to 0.99 g/cm^3, but show a definite trend of fluid densities that are smaller than those predicted for 0.70 to 0.94 g/cm^3.

TABLE OF CONTENTS

ACKNOWLEDGEMENTS

I wish to give recognition to:

My wife and closest companion, judi, for her devoted love and unfailing support throughout our marriage, especially during my studies at the Royal Military College and at the Naval Postgraduate School. You have been a godsend in my life. Thanks for sticking with me. My entire family for their patience and understanding throughout my career in the Navy, in particular the thirteen years I have served at sea.

NPS Faculty. My thesis advisor, Professor Bruce Denardo, for his contagious enthusiasm and solid support throughout the past twelve months and most notably for teaching me as to what is important in research.

Fellow Officer. My friend and mentor, CDR Ed Tucholski, for the significant assistance he has provided me with and for taking the complexity out of physics. It was great to have the privilege to work beside him.

NPS Staff. The entire Department of Physics technical support team. Above all, I must thank two special gentlemen, Mr. Bob Sanders and Mr. George Jaksha, whose efforts were instrumental to the success of this project.

THANK YOU ALL!

Len Pringle

I. INTRODUCTION

The buoyant force on a body that is partially or wholly immersed in a fluid in a gravitational field equals the weight of fluid displaced by the body (Archimedes' Principle). For bodies that are not shaped similar to a canoe or bowl, which can displace more fluid than the volume of the material, the condition for floating is simply that the density of the fluid be greater than the average density of the body. Consider such a body floating in a liquid. The introduction of bubbles results in a fluid whose average density is less than that of the original liquid. If the bubbles are uniformly distributed and small compared to the size of the body, we might expect that the body will sink when the average density of the fluid is less than the average density of the body. However, the bubbles may produce upward forces on the body, due to drag produced by the entrained flows in the fluid and to bubbles sticking to the body. It is thus not clear whether the introduction of bubbles can make a floating body sink. One might argue that the sinking of the body must be possible, because in the limiting case in which the gas displaces all of the water, any object more dense than the gas would sink. But this argument is faulty because it neglects a possibly very large upward drag on the body, which could prevent the body from falling.

The possible sinking due to bubbles has been given as an explanation for the sinking of some ships, especially in the "Bermuda Triangle". This explanation is based on the existence of large amounts of methane gas in the sediments of the region (Rowe and Gettrust 1993). This gas might be disturbed and released

in sufficiently large quantities such that the density of the water is temporarily reduced to levels that a ship cannot displace it own weight of water, and so sinks (McIver 1982). Although it apparently has been established that there is no greater incident of sinkings in the Bermuda Triangle, there is a legitimate scientific issue regarding the sinking of a floating body due to the presence of bubbles. However, we have not found any literature on such an experiment. There has also been some suggestion that the deliberate release of methane hydrate deposits by underwater vehicles could be used to reduce buoyancy and thus sink targets. This is referred to as a "Buoyancy Bomb" (Stumborg, 2000).

Important aspects of the issue are the uniformity of the bubbles and the cross-sectional area over which the bubbles are generated compared to the cross-sectional area of the liquid. Two extreme cases are that (i) the bubbles are generated uniformly over the cross-section of a container, and (ii) the cross-sectional area of the liquid is much greater than that of the bubbles, which would occur in the ocean, for example. In case (i), there can be no net upward flow of liquid, although large-scale nonuniformities in the flow could conceivably occur. In the absence of such flows, there is expected to be little if any drag on a body due to the liquid. In case (ii), large-scale circulation of the liquid will occur, where the liquid rises in the region of the bubbles, and falls outside this region. This is expected to produce a significant upward drag on a body in the region.

The purpose of this thesis is to describe the design and construction of an apparatus that will allow us to experimentally investigate case (i), and to compare the data to theory. We have observed that the upward drag force in case (ii) is

substantial and we recommend that these results be investigated in future work. We show that a body floating in a container of water can indeed be made to sink due to the introduction of small air bubbles uniformly over the cross-sectional area of the container. This offers a dramatic lecture demonstration, which is discussed in Appendix A.

The organization of this thesis is as follows: Chapter II addresses the theory determining the average density of bubbly water at which a body is predicted to sink. The apparatus that we have constructed for this purpose is described in Chapter III. The methods of calibration for our system are provided in Chapter IV. The results of our quantitative investigations, an analysis of the system uncertainties, and a comparison with the theory, are presented in Chapter V. Concluding remarks and suggestions for future work are made in Chapter VI.

THIS PAGE INTENTIONALLY LEFT BLANK

II. THEORY

We require a method of determining the average density of bubbly water. Pure water of volume V_w has mass $\rho_w V_w$, where ρ_w is the density of water. If air bubbles of total volume ΔV are introduced into the water, the average density is then $\rho = \rho_w V_w/(V_w + \Delta V)$, where we neglect the mass of the air compared to the mass of the water. A means of determining this density is to measure the initial height h_o of the water level in the container with no bubbles, and the change in height Δh when the bubbles are turned on and steady state has been reached. If the container has uniform cross-sectional area, then $\Delta h/h_o = \Delta V/V_w$, and so the average density of the bubbly water is:

$$\rho = \frac{\rho_w}{1 + \Delta h/h_o} . \qquad (2.1)$$

We consider the critical value (2.1) of the bubbly water density below which a floating ball will sink. As noted in the Introduction (Ch. I), if bubbles are produced uniformly over the cross-sectional area of a container, there will be no net upward flow of the water and thus no upward drag on the ball. The critical value should then ideally equal the average density of the ball, if there are no large-scale flows. However, above the ball there is a "shadow" region in which there are no bubbles, whereas this critical value assumes that the bubbles are uniformly distributed throughout the entire volume of liquid. To account for the

shadow, we assume that the top of the ball is tangent to the surface of the fluid when the ball is just about to sink. We also assume that the shadow has uniform circular cross sectional area and extends vertically from the equator of the ball to the surface of the fluid, which approximates our observations of the system (Ch. V.A). The volume of the shadow region is easily shown to be $V_S = \pi R^3/3$, where R is the radius of the ball. The absence of bubbles above the ball causes the pressure on the top of the ball to be greater than it would be if bubbles were present. This force is the weight of the additional water above the ball due to the lack of bubbles, so there is a downward force $(\rho_w - \rho)gV_S$ on the ball. Substitution of the above expression for V_S yields the downward force on the ball due to the shadow region as

$$F_S = \frac{\pi}{3}(\rho_w - \rho)gR^3 \ . \qquad (2.2)$$

Because the ball alters the flow of the bubbles, the bubble density near the bottom of the ball and the cylindrical boundary of the shadow region is conceivably greater than that farther from the ball, which may cause a significant additional decrease of the buoyancy. However, our observations (Ch. V.A) reveal that the bubble density is approximately uniform throughout the fluid. The bubbles that would have been in the shadow region are thus effectively uniformly distributed throughout the rest of the water, which reduces the buoyancy by a negligible amount in the typical case where the volume of the water is much

greater than the volume of the ball.

The condition for neutral buoyancy of the ball is $W + F_S = F_B$, where the downward gravitational force is $W = mg$ and the upward buoyant force for a uniform fluid is $F_B = \rho V g$, where m is the mass of the ball and V is its volume. Substituting the expression (2.2) of the shadow force F_S, and solving for the average fluid density ρ, yields the value below which the ball is predicted to sink:

$$\rho = \frac{m + \rho_w \pi R^3/3}{V + \pi R^3/3} . \qquad (2.3)$$

This expression correctly reduces to $\rho_w = m/V$ in the case of no bubbles ($\rho = \rho_w$). We do not set $V = 4\pi R^3/3$ in Equation (2.3) because the ball used in the experiment (Ch. V.A) has a small protrusion as part of the filling hole. The protrusion points downward in the experiment, and causes the volume V of the ball to be 0.6% greater than $4\pi R^3/3$. The ball is also slightly oblate by 0.25%. We minimize the error due to the oblateness by substituting the average radius for R in Equation (2.3).

It should be noted that the above theory predicts that the equilibrium state (in which the top of the ball is tangent to the surface of the fluid) is *unstable*. This occurs because a small downward displacement of the ball causes the downward force due to the shadow to increase, but does not alter the buoyant force for a uniform fluid.

THIS PAGE INTENTIONALLY LEFT BLANK

III. APPARATUS

In this chapter we describe the design and construction of the apparatus used to produce a volume of bubbly water. As shown in Figure (3.1), the main components of the apparatus are a cylindrical acrylic chamber and an array of bubble diffusers. The diffusers are connected to a pressurized nitrogen gas cylinder through a manifold and a series of control valves, and generate a controllable volume of nitrogen bubbles.

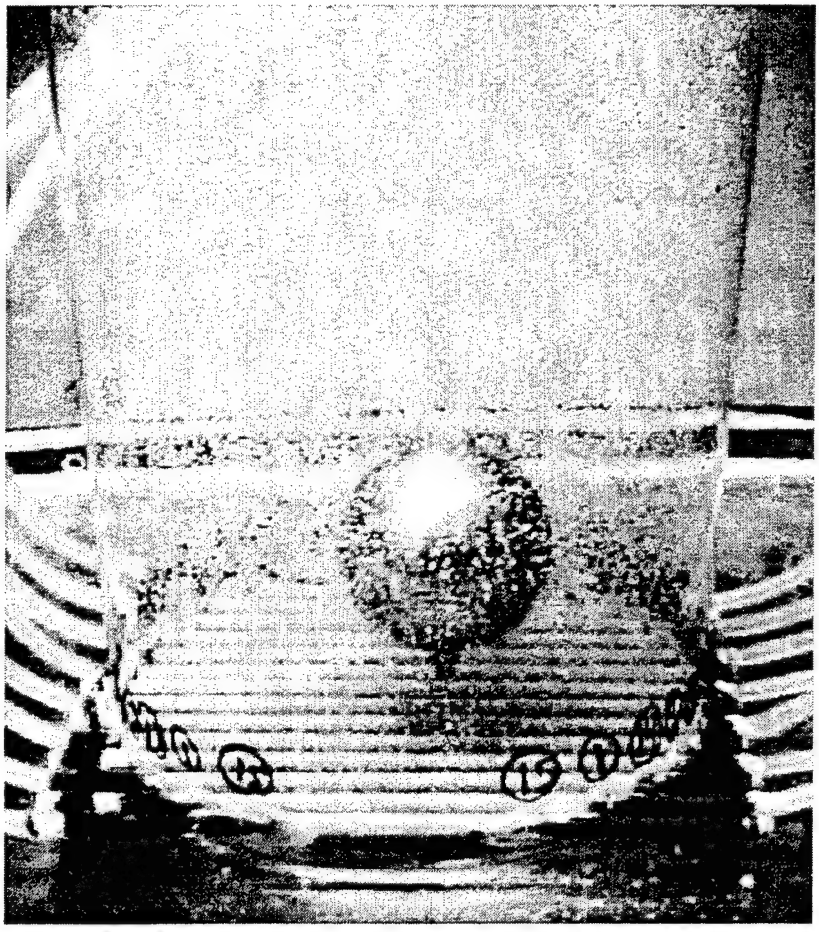

Figure 3.1. Main components of the apparatus: a cylindrical acrylic chamber, and an array of 15 bubble diffusers. Also shown is the buoyant body, which was employed throughout the thesis. The body has been sunk due to bubbles. To avoid distortion, this picture was taken with the chamber submerged in a large reservoir of water.

A. THE BUBBLY WATER CHAMBER

The bubbly water environment is created within an acrylic tube that is closed at the bottom and open at the top. The dimensions of the tube are 30.6 cm for inner diameter and 60 cm in height with a wall thickness of 3.175 mm. The water depth is maintained at approximately 40 cm to allow for a nearly 20 cm increase in height resulting from the introduction of the bubbles.

The chamber's cylindrical shape was selected to minimize the wall surface area for a given volume and thus minimize the surface drag of the bubbles on the walls of the chamber. The cylindrical shape also provided no corners that might needlessly complicate the bubble flow pattern. The diameter of the chamber was chosen to be as large as conveniently possible compared to the diameter of the buoyant body. The chamber height allows for a uniform mixing of the bubbles ensuring an equal distribution of the small air bubbles over the cross-sectional area of the chamber. The clear acrylic material facilitates viewing and photography of the bubbles and the buoyant body.

Holes of diameter 0.7 cm were drilled 3 cm from the bottom of the chamber to allow 15 bubble-generating diffusers to penetrate the cylinder. The holes were placed such that the diffusers were evenly spaced and parallel to each other (Fig. 3.2). To determine where to place the holes, we required the arc length to the center of diffuser from an initial point on the tube. This was found to be:

$$ArcLength(N) = R_T Cos^{-1}\left[\frac{R_T - (t_T + d_T + D_d + NS_d)}{R_T}\right], \qquad (3.1)$$

where R_T = tube radius (OD) = 153 mm, t_T = tube thickness = 3.175 mm, d_T = distance of the 1st diffuser from the chamber wall = 4 mm, D_d = diffuser diameter = 5.6 mm, N = diffuser number = 1 –15, and S_d = distance from center to center of diffusers = 20 mm.

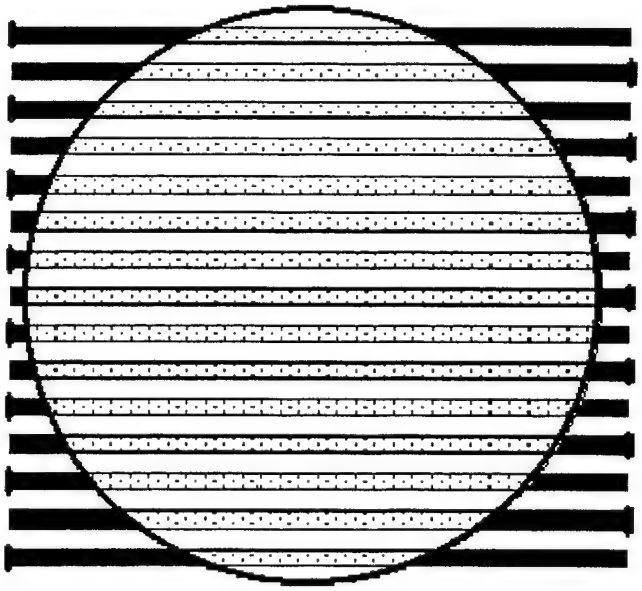

Figure 3.2. Top view of the bubbly water chamber and diffuser arrangement.

A 6 mm thick acrylic plate, 33 cm square, was glued to the bottom of the tube. Once the diffusers were inserted into the holes, the plate effectively created a chamber that was both water and air tight below the water line. This proved to be an important feature during the acquisition of the experimental data (Ch. V.A).

B. VOLUMETRIC BUBBLE GENERATOR

Several bubble making devices, including perforated coiled flexible tubing, "frits" and perforated acrylic plates, were considered prior to the final selection being made. The three primary criteria for the diffuser selection were: the bubbles must be much smaller than the buoyant body yet large enough so that direct absorption of the nitrogen gas into the fluid is inhibited; there must be a constant and diffused flow of bubbles to ensure a uniform distribution over the cross-sectional area of the chamber, reducing possible fluid turbulence; and the diffusers must be sufficiently robust to physically withstand a large volumetric flow of nitrogen over extended periods. The device that provided the most uniform bubble field, with small diameter bubbles and little turbulence, was a set of aquarium diffusers (Regent PL-T714). The diffusers are hollow porous tubes capped at one and with an air inlet at the other. The dimensions of the diffusers are 36 cm in length, 5.6 mm in diameter and a wall thickness of .75 mm.

A visual examination of individual Regent diffusers showed a wide variation of performance between diffusers, both in pattern flow and in bubble size. A Canon Optura digital video camera was employed to examine the flow of 25 individual diffusers, for longitudinal uniformity and bubble size uniformity. Fifteen diffusers were selected from this lot and strategically positioned to give the most uniform cross-sectional flow pattern possible. The diffusers were inserted through the chamber holes (Sec. A). The portion of the diffusers that extended outside of the chamber was made water and air tight through the use of

heat shrink and silicon sealant.

C. NITROGEN GAS FEED SYSTEM

A schematic of the feed system is shown in Figure 3.3. Accurate control of the volume flow rate to the diffusers was important. Overall gas flow rate was controlled with a single stage pressure regulator (Matheson Gas Products Model 1L-580) in conjunction with an inline flow meter. Tygon tubing (0.3125 in ID) connected the nitrogen source to individual diffuser control valves (Copper - 9075656) through a manifold (locally fabricated). Balancing of the diffuser control valves was found to be critical in the stability of the generation of bubbles. Any small deviation from a perfect balance set up substantial turbulent flow in the chamber (Ch. IV.A.5). It is recommended that multi-turn needle valves be utilized in the future to replace the inexpensive gate valves that we employed.

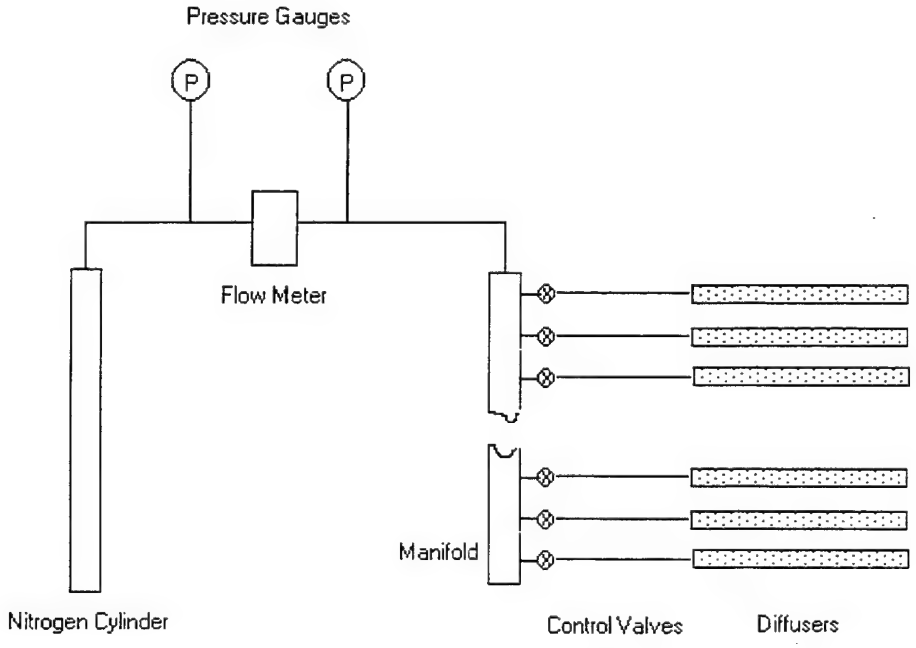

Figure 3.3. Schematic of the nitrogen gas feed system. There are 15 diffusers.

THIS PAGE INTENTIONALLY LEFT BLANK

IV. METHODS AND SYSTEM CALIBRATION

A. METHODS

As explained in Chapter II, if air bubbles of total volume ΔV are introduced into the water, the average density is $\rho = \rho_w V_w/(V_w + \Delta V)$. The ability to accurately determine the density of the bubbly water was critical to our experiment. A method that consistently provided a means to accurately determine the density proved to be a challenge and required several evolutions. Five different methods to determine the average density of the bubbly water were attempted, one with very good outcomes, others with limited or negligible results.

1. Bubble Velocity Method

The volume of gas that passes through the flowmeter in a certain amount of time T is the product of the volume flow rate Q and the time. When considering the volume of gas ΔV contained in the bubbles in the water, the relevant time is that required for the bubbles to rise from the bubble generators to the surface. To determine ΔV, we note that, as a result of viscous losses in the tubes and manifold, the pressure p_f at the flowmeter is greater than the pressure at the bottom, which is approximately atmospheric pressure p_o. We make the assumption that the air remains at constant temperature as it flows, so that the product of pressure and volume is constant (Boyle's law). This yields $p_f QT = p_o \Delta V$. Solving for ΔV yields:

$$\rho = \frac{\rho_w}{1 + p_f Q T / p_o V_w}. \qquad (4.1)$$

Equation (4.1) allows the average density of bubbly water to be calculated from parameters that can be measured.

A digital video camera (Canon Optura) was employed to capture the time-distance sequence of a typical bubble of 2 mm diameter. A meter stick photographed in the plane of the bubble provided the distance scale factor for the evaluation of displacement and size. The average vertical speed was found to vary from 25.2 to 34.3 cm/s depending on the flow rate. This is consistent with Morton (1953) who concluded that a single 2 mm bubble reached a velocity of 24 cm/s in water, and that the presence of wake in the liquid (caused by other bubbles in close proximity) results in higher velocity of rise of the bubble. Our bubble velocity method proved to be accurate only to a volume flow rate of 3 l/min, at which the larger quantity of bubbles made it very difficult to discern one bubble from another. The 3 l/min flow rate represented only about 2% of the expected range of our experiment. The problem is that we cannot assume that the bubble velocity is independent of flow rate, because the bubble size may change, and the bubbles may interact. Therefore other methods needed to be explored.

2. Trailing Edge Method

An alternative approach to the above method was attempted. We measured the rise time T by stopping the airflow and timing the trailing edge of

the bubbles as it passed from a lower plane to the surface. Although the bubble diameters averaged 2 mm, they in fact ranged from 0.5 mm to 3 mm and consequently the different velocities made a discrete trailing edge too difficult to distinguish.

3. Acoustical Method

The speed of sound in a fluid is given by:

$$c^2 = \frac{B_{ad}}{\rho} = \frac{1}{\rho \kappa_{ad}}, \tag{4.2}$$

where B_{ad} is the adiabatic bulk modulus, ρ is the mass density and $\kappa_{ad} = B^{-1}{}_{ad}$ is the adiabatic compressibility of water (Crocker, 1998). If an amount of undissolved nitrogen gas is uniformly mixed with water, the mixture may be treated as a homogenous fluid for sufficiently large wavelength. Equation (4.2) may then be applied, where the density and compressibility are the volume-weighted averages of the gas and the liquid densities and compressibilities:

$$\rho = x\rho_g + (1-x)\rho_l, \tag{4.3}$$

$$\kappa_{ad} = x\kappa_g + (1-x)\kappa_l. \tag{4.4}$$

Here the subscripts g and l refer to gas and liquid, respectively, and x is the gas volume fraction. Substituting Equations (4.3) and (4.4) into Equation (4.2)

and solving for x yields:

$$x = \frac{\sqrt{c^2(\kappa_g^2\rho_l^2 - 2\kappa_g\kappa_l\rho_g\rho_l + \kappa_l^2\rho_g^2) + 4(\kappa_g - \kappa_l)(\rho_g - \rho_l)} - c(\kappa_g\rho_l + \kappa_l(\rho_g - 2\rho_l))}{2c(\kappa_g - \kappa_l)(\rho_g - \rho_l)}, \quad (4.5)$$

Equation (4.5) allows x to be determined by measuring c.

A point source transducer (USN DT-574/BQQ-6) was driven by a 3-pulse burst from a 15 MHz Function/Arbitrary Waveform generator (HP 33120A) through a power amplifier (HP 467A) at the transducer's resonant frequency of 26.65 kHz. Two pickup hydrophones (EDO Model 6600) were positioned in line with the source beam. The receive signals were recorded on an oscilloscope (Agilent Infiniium 54810A) through low noise pre-amplifiers/filters (Stanford Research Systems Model SR 560). Knowing the distance between the hydrophones and measuring the time between the two received waveforms allow us to easily determine the speed of sound in water without bubbles. However, when bubbles were introduced into the water, a frequency spectrum shows a loss greater than 70 dB in the received signals and as such the transmitted signal became 'buried' in the ambient noise. Increasing the source level and further amplifying the received signal provided no further assistance in raising the receive signal out of the noise.

We ruled out attenuation of the signal due to resonance frequency which is:

$$f_o = \frac{1}{2\pi a}\sqrt{\frac{3\gamma P_b}{\rho_o}} \qquad (4.6)$$

with a = bubble radius, ρ_o = density for water, γ = specific heat constant and $P_b = P_o\,(1 + z/10)$ for z in meters (Kinsler et al. 2000). For our average 2 mm diameter bubble, at a depth of 10 cm, the resonant frequency is 3.28 kHz, which is much less than the 27 kHz frequency of the sound. The lack of signal at the pickup hydrophones could be due to ineffective coupling of the driving transducer into the medium, or to the scattering of the sound waves off the bubbles or turbulence caused by the bubbles. This technique was thus ruled out as an inaccurate means of measuring the density of our bubbly water.

4. Dielectric Material Method

By measuring the capacitance C of a parallel plate capacitor with the space between the plates having area A filled with bubbly water and the capacitance C_w with water between the plates, we can find the average density of the bubbly water in the chamber. From the relationship of capacitance $C = \frac{\kappa_d \varepsilon A}{d}$, where ε is the permittivity of free space, Equation (4.3), and $\kappa_d = x\kappa_g + (1-x)\kappa_l$, we find:

$$\rho = \rho_w \frac{C}{C_w}, \qquad (4.7)$$

where κ_g and κ_l is the dielectric constant of the gas and liquid respectively, and with the understanding that $\kappa_l >> \kappa_g$, and $\rho_l >> \rho_g$.

To acquire an accurate average density of the bubbly water, it was estimated that the plates would have to be at least 15 cm apart. With this plate separation, the largest plate area that would fit into the chamber was calculated to be 600 cm^2. The theoretical capacitance of water for a parallel plate capacitor with the above parameters is 273 pF.

A preliminary test to determine the practicality of this method was conducted. Two unetched, copper clad printed circuit boards, with dimensions 20 cm x 30 cm, were placed in parallel and 25 cm apart on the outside walls of a glass aquarium. The aquarium was filled with water. The copper plates were connected to an impedance analyzer (HP 4194A) using a two-terminal measurement configuration. The results of our test were inconsistent with theory and did not vary greatly when bubbles were introduced to the water. We attributed this to two assumptions in Equation (4.7): the space between the plates is filled with a homogenous dielectric; and the plate separation is small compared with the dimensions of the plate. The latter would allow the fringing field of the plates to be ignored. Both of these assumptions were violated in our test set up and it was predicted that similar results could be expected if employed in the chamber. This technique was also ruled out as an accurate means of measuring the density of our bubbly water.

5. Change in Height Method

A standard means of determining the density of bubbly water is to measure the initial height h of the water level in the chamber with no bubbles, and the change in height Δh when the bubbles are turned on and steady state has been reached. If the container has uniform cross-sectional area the average density of the bubbly water can be determined from Equation (2.1).

We found that we were able to accurately measure the change in height only after the diffusers were in perfect balance; that is, the flow rate per unit length was identical over each diffuser. When slightly out of balance the bubble flow became very turbulent, eddies were observed within the volume of bubbly water and the surface took on a boiling like appearance. We were then unable to measure the change in height with any sort of precision.

The nitrogen source originally fed all the diffusers from the same direction. Visually it appeared that there was a greater flow of bubbles stemming from the source end than from the opposite end. By alternating the source direction for every other diffuser the turbulence was reduced significantly. Further reduction was accomplished by meticulously adjusting each of the 15 control valves such that the bubble flow from each diffuser was visually balanced. The bubble flow became uniform throughout, the eddies completely disappeared, and the surface became level.

B. SYSTEM CALIBRATION

The ability to accurately measure the change in height (Sec. A.5) allowed us to use Equation (2.1) to determine the density of the bubbly water. To simplify this procedure we calibrated the change in height Δh as a function of the total gas flow rate Q. Flow rates ranging from 0 to 134 l/min, at 15 different values, were set at the nitrogen source, and the corresponding changes in height were recorded. Three different flowmeters were required to cover the range of interest. Two 150-mm direct-reading flowmeters (Gilmont Instruments) covered the lower range 0 – 16 l/min (GE717) and 16 – 44 l/min (GE817), and a digital flow sensor (McMillian 100-18 Flo-Sen) was employed at the higher flow rates. The results of the system calibration are shown in Figure 4.1. A 3rd order polynomial was used in a least squares fit through the points, resulting in:

$$\Delta h = a + b_1 Q + b_2 Q^2 + b_3 Q^3, \tag{4.8}$$

where $a = -0.171507$, $b_1 = 0.419662$, $b_2 = 3.330407 \times 10^{-4}$, and $b_3 = 3.297877 \times 10^{-5}$. The flow rate Q is measured in l/min and change in height Δh is measured in mm.

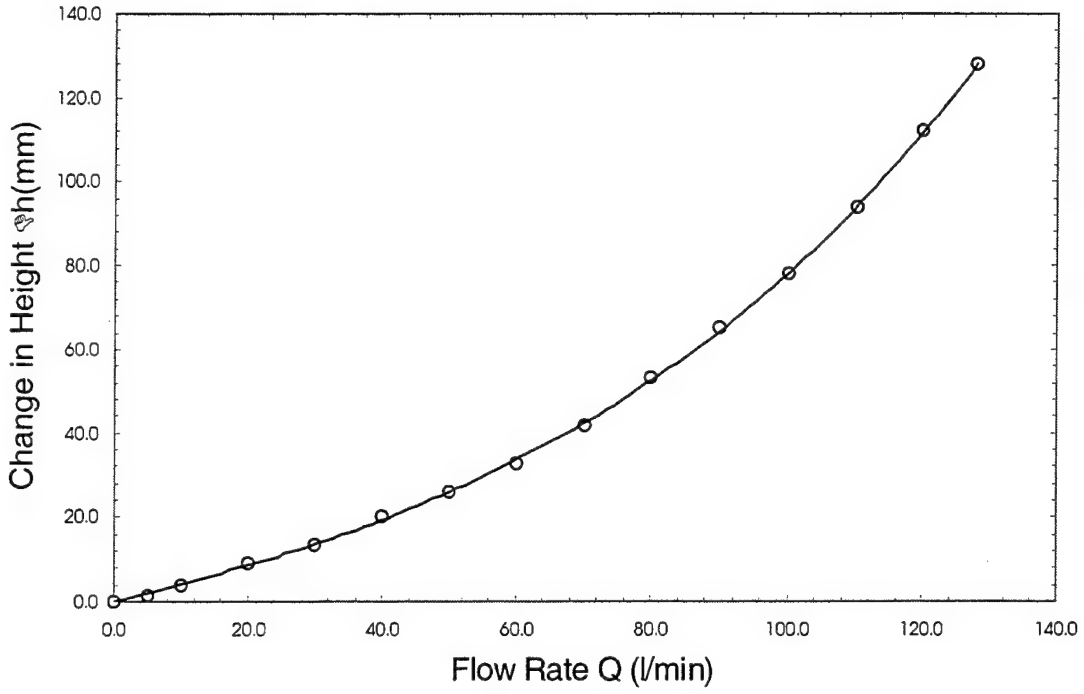

Figure 4.1. Change in surface height vs flow rate at the nitrogen source. The curve is a 3rd order best fit polynomial.

THIS PAGE INTENTIONALLY LEFT BLANK

V. EXPERIMENT

Our objective in the experiment is to make a buoyant body sink by adding bubbles, and to gather the data needed to use Equation (2.1) to calculate the density of the fluid when this occurs. We conduct an error analysis on the system and finally discuss the results of our findings.

A. EXPERIMENT

We required a buoyant body that was much larger relative to the bubbles so that we could treat the effects of the bubbly water on the object as those of a homogenous fluid. We selected a commercially available "density ball", which is a hollow, stainless steel, 101.3 mm diameter sphere with a removable plug (Cenco Scientific Co. cat. #76595N). Liquid can be added or removed to vary the ball's mass and thus its average density. We employed mineral oil in order to prevent rusting.

We obtain an accurate value of the volume of the ball by a variation of Archimedes' method (weighing a body in and out of water). Sufficient liquid is added to the ball such that it will sink in water. We then place a container of water on a digital balance (AND Electronic Balance FX-2000), and "zero" the balance. The ball is suspended by string from a support and is totally immersed in the water without touching the container. We record the reading m of the scale. The buoyant force mg equals the weight $\rho_w V_{ball} g$ of the displaced water, so the volume of the ball is $V_{ball} = m/\rho_w = 556.73\ cm^3$. This method has two

advantages over Archimedes' method: arranging suspension of a body from an elevated balance is avoided, and the buoyancy due to air is irrelevant. The mass of the empty ball is 229.61 g, so the minimum average density of the ball is 0.4124 g/cm^3.

For the main part of the experiment, we determine the average density of the bubbly water required to sink the ball. We select an amount of liquid in the ball such that it floats in the water. We place the ball in the chamber, slowly increase the flow rate Q, and record the minimum value for which the ball sinks below the surface. We then compare this to the ball's average density, which is determined as the total mass (including liquid inside) divided by the volume of the ball. The entire process is then repeated for a different value of the average density of the ball.

In our initial experiments, we observed two effects that cause deviations from the measured values of the requisite airflow rates, but which could be eliminated. First, bubbles sticking to the lower half of the ball effectively lower the ball's average density, which make the ball neutrally buoyant at a higher airflow rate than expected. Second, when the ball is floating at the surface, there is a meniscus that forms around the ball at the ball-water interface, so surface tension is acting upward on the ball. This force must be overcome with a higher airflow rate when sinking the ball. The number of bubbles sticking to the surface of the ball was reduced to nearly zero by machine polishing the ball and thoroughly cleaning it with isopropyl alcohol prior to each trial. Considerable care was also taken when handling the ball to prevent any fingerprints on the surface.

We substantially reduced the surface tension by applying to the outer ball surface a very thin coat of Photo-Flo 200, which is a surfactant used in film developing. Another effect, the absence of bubbles above the ball, could not be eliminated, so we incorporated estimations of this effect into the theory (Ch. II).

The criterion we set for determining the sinking of the ball was that it remain below the surface of the water for roughly 70% of the time over a 30 second period. This benchmark was necessary to define the sinking of the ball because as the fluid density approached the density of the ball, the ball tended to "loiter" in a volume of bubbly water just below the surface of the water rather than sinking directly to the bottom. Occasionally, during this loitering phase, the ball would subtly break the surface of the water.

Figure (5.1) shows the results of an experiment to determine the average fluid density at which the ball sinks. The fluid density at which the ball just sinks below the surface is significantly greater than the density of the ball, which is represented by the identity line in the graph. A 3rd order polynomial was used in a least squares fit through the points, resulting in:

$$\frac{\rho}{\rho_w} = c + d_1 Q + d_2 Q^2 + d_3 Q^3, \tag{5.1}$$

where $c = 0.999826$, $d_1 = -8.694053\times10^{-4}$, $d_2 = -4.972911\times10^{-6}$, $d_3 = -2.06743\times10^{-8}$, and where Q is measured in l/min.

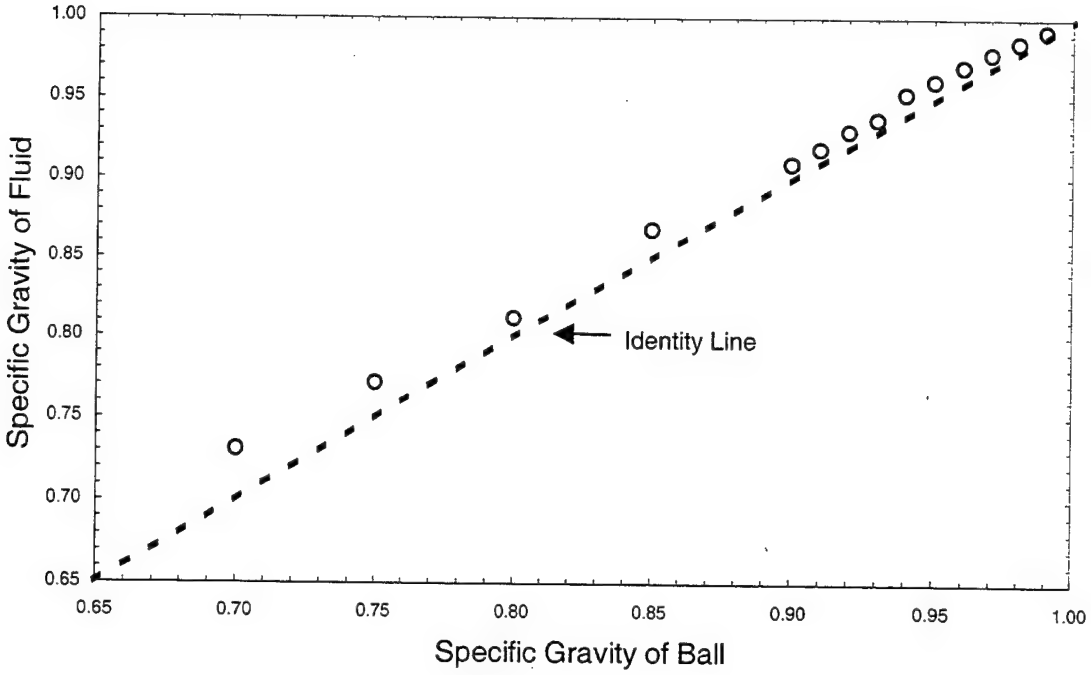

Figure 5.1. The fluid density at which the ball just sinks below the surface is significantly *more* than the density of the ball, which is represented by the identity line in the graph.

Several special observations were noted during our experiment. First, it appeared to all observers that the volume fraction of bubbles was much greater than what it actually was, judging solely by the vast number of bubbles in the chamber. Only after determining the actual density using the change in height method (Ch. IV.A.5) was an observer convinced that his or her visual intuition was incorrect. Second, as the flow rate increased above 5 l/min the bubble velocity decreased. This is contrary to Morton's (1953) observation that bubble velocity increases in the presence of wake. Solving for T in Equation (4.1), the bubble velocity $v = (h_o + \Delta h)/T$ results in our finding shown in Figure (5.2). Third, when the top of the ball is tangent to the surface of the fluid, there exists a shadow above the ball in which there are no bubbles. The shadow has a uniform

circular cross-sectional area that extends vertically from the equator of the ball to the surface of the fluid. Once the ball is sunk the "plume" bulges outward.

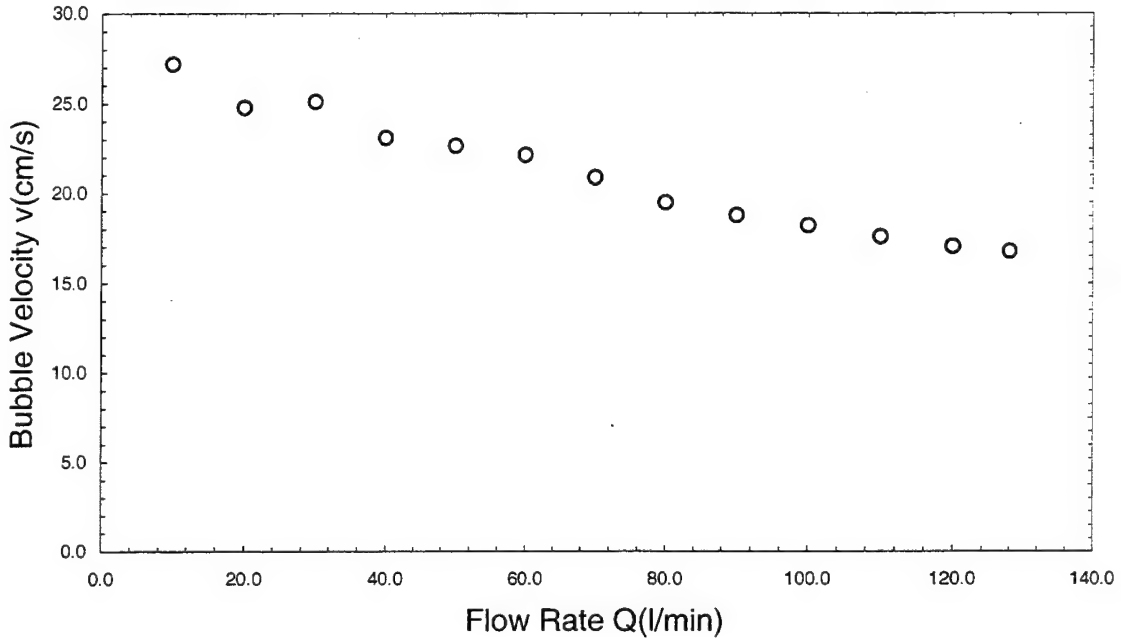

Figure 5.2. Above 5 l/min the bubble velocity decreased which is contrary to Morton's observation that bubble velocity increases in the presence of wake.

B. ERROR ANALYSIS

There are a number of sources of error in the determination of the density at which the ball sinks. Uncertainties exist in the flowmeters outputs, the measurement in the change of the surface height, and the flow rate at which the ball sinks below the surface. In this analysis, all uncertainties are worst-case tolerances.

We first consider the system calibration (Ch. IV.B), for which there are

three independent contributions to the uncertainty: the repeatability of the flowmeter, the resolution of the flowmeter, and the uncertainty δh in measuring the surface height after the introduction of bubbles. Both the repeatability and resolution are taken directly from the flowmeter manufacturers' specifications (App. B). The Gilmont flowmeters are flow rate dependent. The McMillian flowmeter is not. Although we found the surface to be level during system calibration, there is some uncertainty when measuring the surface height h. This we determined to be $\delta h = \pm 0.5$ mm regardless of flowrate Q. The result of our system calibration error analysis is shown as error bars in Figure 5.3.

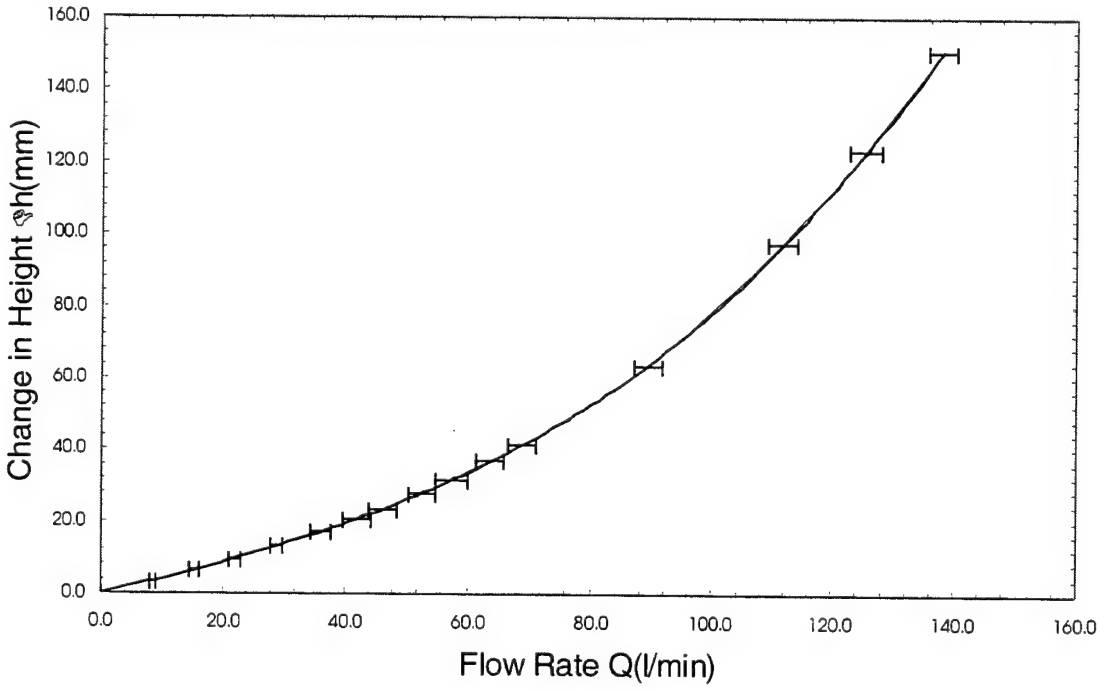

Figure 5.3. Calibration curve for the change in height Δh as a function of the flow rate Q. Independent uncertainties exist in Δh directly and in Q. The latter indirectly causes an uncertainty in Δh, which is negligible on the scale of the figure.

We next consider the experiment (Sec. A), in which we determine the

specific gravity of the fluid at which the ball sinks. There is one independent contribution to the uncertainty: the repeatability of the experiment. Seven separate trials were conducted for a given specific gravity of the ball. The flow rate for which the ball sinks below the surface was recorded each time. The uncertainty in the experiment repeatability was calculated as half of the difference between the maximum and minimum flow rates recorded.

The overall uncertainty in the flow rate δQ is the quadrature sum of the flowmeter repeatability, the flowmeter resolution, and the experiment repeatability. The error bars in Figure 5.4 show the uncertainty of the specific gravity of the fluid, which is a direct function of the uncertainty in the change in height $\delta(\Delta h)$, and is determined by:

$$\delta(\Delta h) = \sqrt{(\delta h)^2 + (\partial f(\Delta h)/\partial Q)^2 (\delta Q)^2}, \qquad (5.2)$$

where $f(\Delta h)$ is a 3rd order polynomial least squares fit (Eq. 4.8), and where the uncertainty of the specific gravity is:

$$\frac{\delta\rho}{\rho_w} = \frac{1}{(1 + \Delta h/h_o)^2} \frac{\delta(\Delta h)}{h_o}. \qquad (5.3)$$

Definitions, specifications of flowmeters, and detailed results of uncertainties are provided in Appendix B.

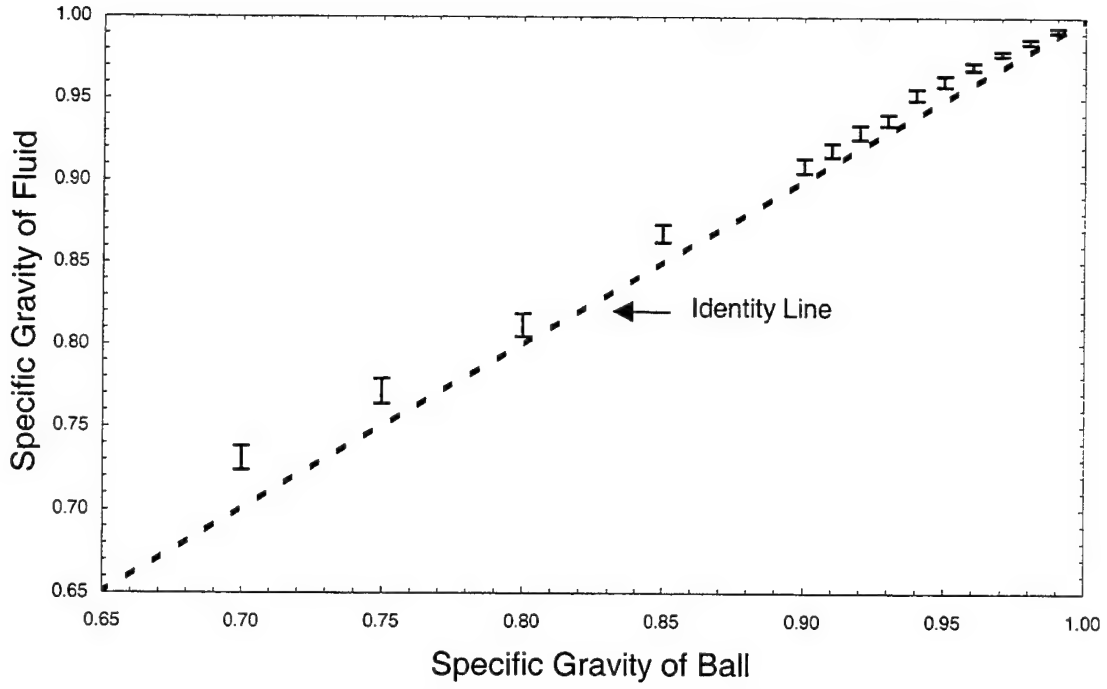

Figure 5.4. Uncertainty of the specific gravity of the fluid is a direct function of the uncertainty in the change in height $\delta(\Delta h)$.

C. SUMMARY OF FINDINGS

The results of our experiment clearly shows that the fluid density at which the ball just sinks below the surface is significantly greater than the density of the ball, which is represented by the identity line in the graph (Fig. 5.4). The experimental data, which include the quantitative error analysis, agree well with the theory for average ball densities from 0.94 to 0.99 g/cm^3, but show a definite trend of fluid densities that are smaller than those predicted for 0.70 to 0.93 g/cm^3 (Fig. 5.5 and 5.6).

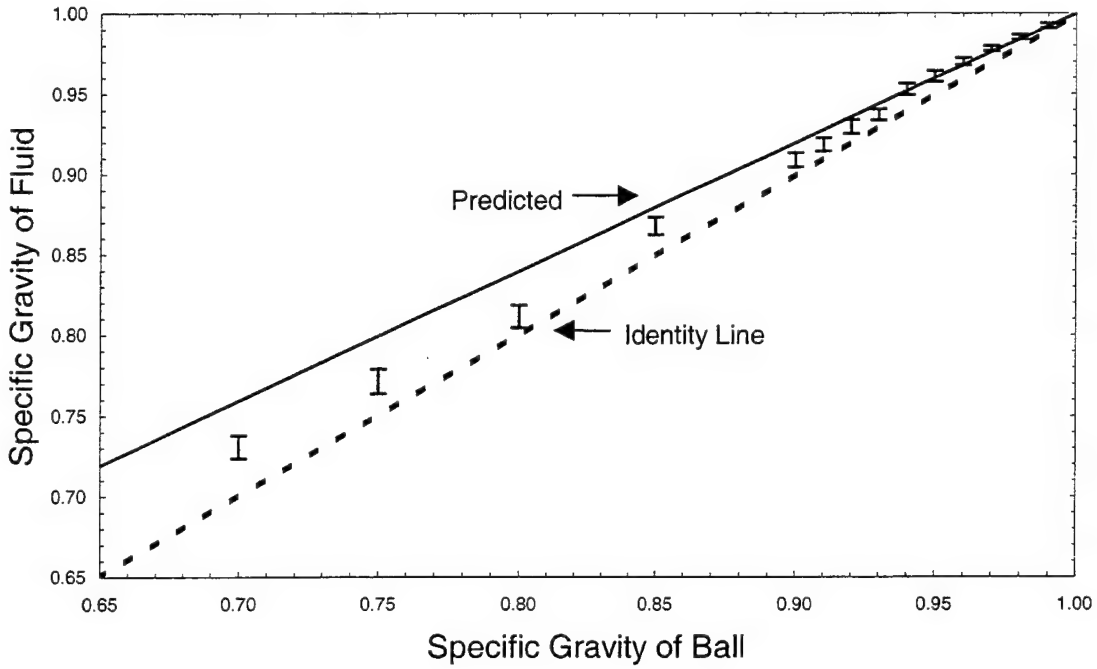

Figure 5.5. The fluid density at which the ball just sinks below the surface is significantly greater than the density of the ball, which is represented by the identity line in the graph. The experimental data agree well with the theory for specific gravity of the ball from 0.94 to 0.99, but show a definite trend of fluid densities that are smaller than those predicted for 0.70 to 0.93.

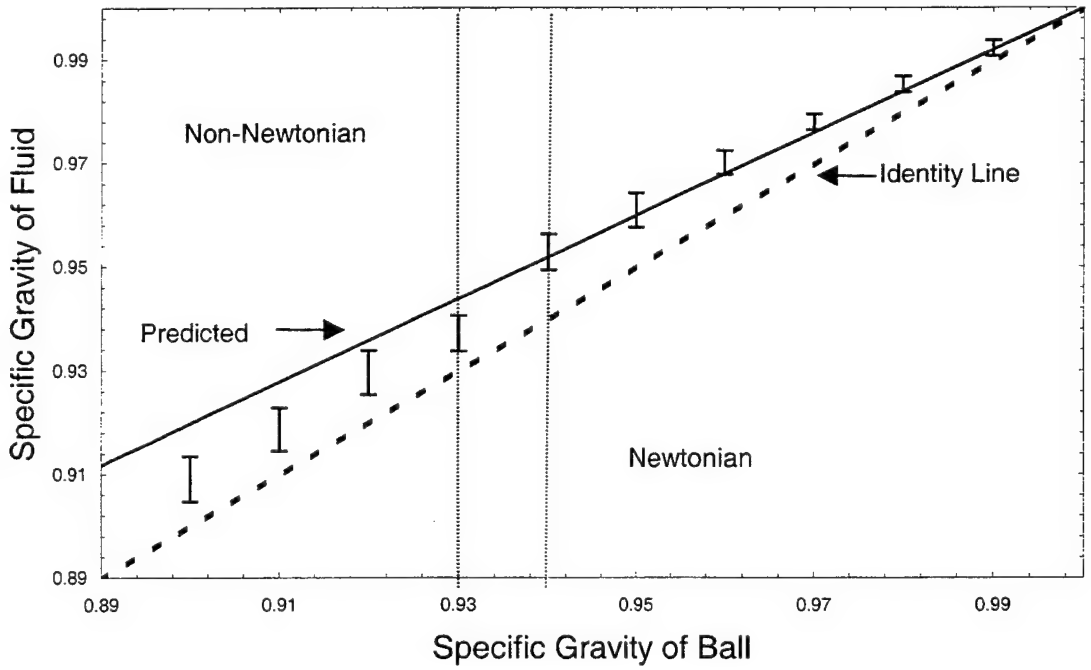

Figure 5.6. An expanded view of Fig (5.5), showing the region of transition from dilute Newtonian fluid behavior to possibly non-Newtonian fluid.

We consider two possibilities for this abrupt transition between 0.94 – 0.93 g/cm^3. First we suspect that there may exist large-scale nonuniformities in the flow as discussed in Chapter I. To investigate, we placed in the chamber a spherical body that is much smaller than the chamber diameter and with a density of 0.91 g/cm^3. We slowly increased the flow rate Q and stopped a number of times prior to the body actually sinking. During these stopped times we carefully observed the response of the body as it explored the cross-sectional area of the chamber. No changes in the water depth of the body were witnessed thus we conclude that there are no large-scale nonuniformities in the flow. Second we speculate that the abrupt transition may be linked to a change of flowmeters near the flow rate region of interest. However, a third flowmeter (McMillian 100-13 Flow-Sen) covering a range of 20 – 100 l/min was employed to verify previous data. The results were nearly identical thus we deduce that the change of flowmeters was not the cause.

The abrupt transition may be attributed to a change from Newtonian to non-Newtonian behavior of the fluid (Wallis, 1969). At low flow rates, we can treat the fluid as simply diluted water and our prediction holds; however, at higher bubble concentrations the mixture tends to rapidly become non-Newtonian, exhibiting a yield stress, and a decreasing apparent viscosity with increasing shear rate. Wallis states that this transition occurs at void fraction above about 0.05 (Specific Gravity = 0.95). We believe to have acquired empirical data to support the theory and although we consider our findings to be very interesting, further investigation is outside the scope of this thesis and we recommend it for future work.

VI. CONCLUSIONS AND FUTURE WORK

A. CONCLUSIONS

In our experimental investigation we show that the introduction of gas bubbles into a liquid decreases the average density, and thus decreases the buoyant force on a floating body. We investigated the critical average density required to sink a buoyant body in water with bubbles. A theory of the critical density for sinking was developed, and predicted that the average fluid density is greater than the ball density for sinking. The experimental data, which include a quantitative error analysis, agreed well with the theory for average ball densities at low flow rates, but show a definite trend of fluid densities that are smaller than those predicted for high flow rates. This may be due to the abrupt onset of non-Newtonian behavior of the fluid.

B. FUTURE WORK

This research would benefit from substantial further study. This thesis investigated the bounded case where bubbles are generated uniformly over the cross-section of a container. Follow on research could investigate the case where the cross-sectional area of the liquid is much greater than that of the bubbles, which would occur in the ocean, for example. A preliminary qualitative experiment showed that a far greater flowrate was required to sink the body in a

more open environment then was needed during our experiment. Also the transitional region should be further investigated to confirm our speculation that it is indeed a change from Newtonian to non-Newtonian fluid characteristics.

APPENDIX A. DEMONSTRATIONS

Our investigations of the introduction of bubbles to sink a body floating in a liquid naturally began with ice and water. We were partly motivated to do this as a dramatic lecture demonstration that would impress introductory physics students. We employed a specially designed acrylic cylinder of height 2.0 feet and inner diameter 3.0 inch (Fig. A.1). The cylinder is open at the top and closed at the bottom, and has an air inlet below an acrylic plate that is 4.0 inches from the bottom. Drilled through this plate are 97 holes of diameter 1/32 inch, and uniformly spaced 1/4 inch apart. It should be noted that the air chamber beneath the plate can be pressurized before water is added to the cylinder, in order to prevent the water from leaking through the holes. An alternative is to close the air inlet with a valve, because water then enters the chamber at a sufficiently slow rate that there is ample time to perform the demonstration.

Ice cubes roughly 1 inch on a side were used. To be visible to more than a small audience, the ice should be prepared with red food coloring or dye. With the apparatus, we are able to sink the ice with sufficient flow from a compressed air cylinder. However, after the ice sinks, it continues to bob up and down due to turbulence, and occasionally even returns to the surface for a short time. The demonstration is more easily and convincingly performed with a body whose average density is very near that of water. Such a body sinks at a lower flow rate, which causes less turbulence. In addition, the air can be simply supplied from the demonstrator's lungs to sink the body. A small closed bottle that has

been appropriately weighted works well.

Permanent sinking can be shown by using a body similar to a boat, in which the material of the body has an average density greater than that of water. For example, a metal cap from a bottle can be employed. However, it is not clear that the sinking in this case is due to a lowering of the average density due to the bubbles, because the substantial foaming that occurs on the surface causes water to collect inside the cap.

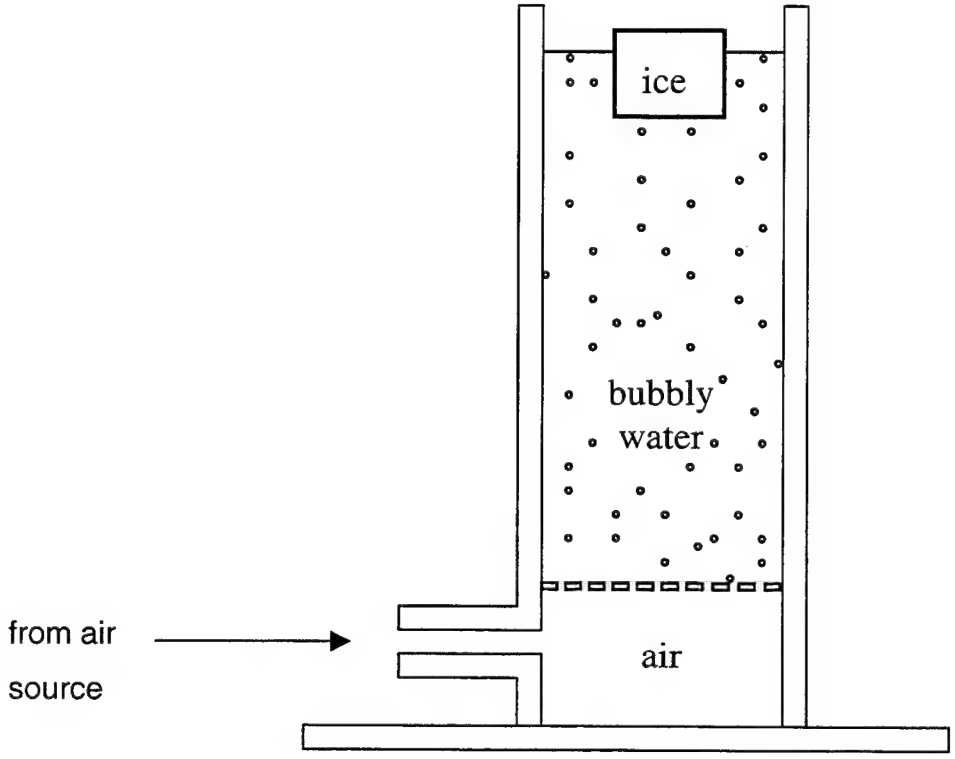

Figure A.1. Original apparatus employed to sink a cube of ice with the introduction of bubbles.

Motivated to construct an apparatus that is more easily observed and controlled, we used a commercially-available "density ball," which is a hollow,

stainless steel, 10.2 cm diameter sphere with a removable plug so that liquid can be added or removed to vary the ball's mass and thus its average density (Cenco Scientific Co. cat. #76595N). Because the ball was too large to fit in the above apparatus, we experimented with several other bubble-making devices in larger containers. These "bubblers" included coiled flexible tubing in which small holes were made by puncturing, and "frits" (aggregates of small clumps of metal). The apparatus that provided the most uniform bubble field with little turbulence and small bubbles was a set of four aquarium bubblers, (Regent PL-T714) which are hollow porous tubes capped at one end and with an air inlet at the other (Fig. A.2). We cut appropriate lengths to span the bottom of a 4.0-liter beaker. The bubblers are held on the bottom of the beaker with suction cups that clip onto the bubblers. Air is supplied by a compressed air cylinder through a pressure regulator, and distributed with a four-way controllable manifold designed for aquarium use. By adjusting the average density of the ball to be a few percent less than the density of water, we are able to sink the ball with a flow rate sufficiently low to cause little turbulence. When the density of the ball is less than about 95% of the density of water, flow rates high enough to sink the ball cause noticeable turbulence. This apparatus functions well, and can be observed even in a large lecture hall.

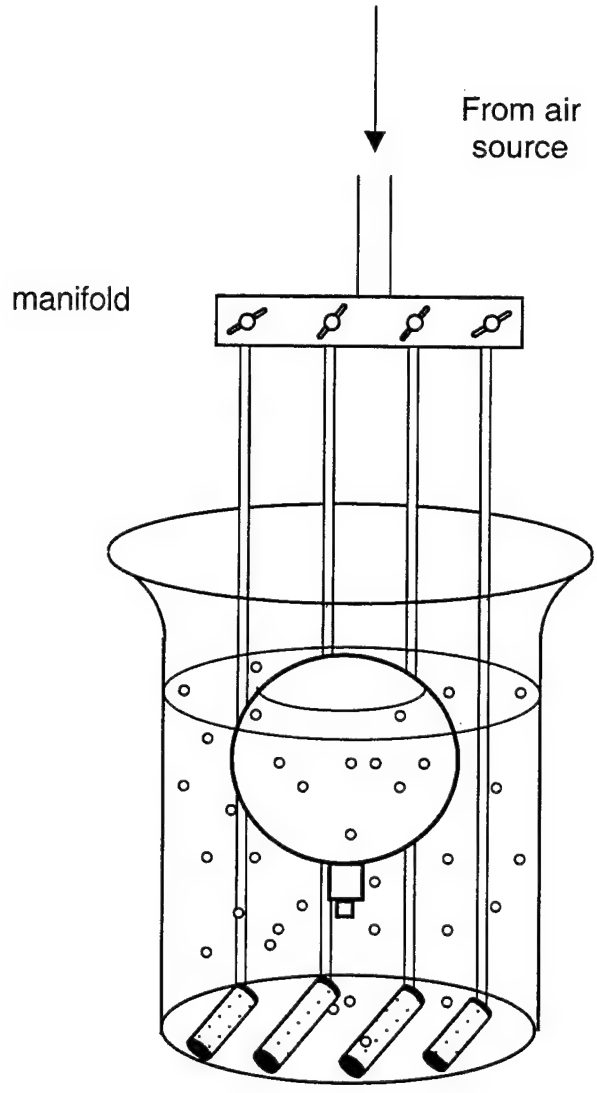

Figure A.2. Subsequent apparatus that can be observed even in a large lecture hall.

APPENDIX B. ERROR ANALYSIS DETAILS

I. FLOWMETER SPECIFICATIONS

Table B.1 provides the flowmeter specifications that are used in the error analysis.

Manufacturer	Flow Rate Range (liters/min)	Repeatability	Resolution (liters/min)
Gilmont	0 - 16	± 0.25% Reading	± 0.25
Gilmont	0 - 44	± 0.25% Reading	± 0.25
McMillian	40 - 200	± 1% Full Scale	± 0.50

Table B.1. Flowmeter Specifications.

II. COLUMN DEFINITIONS

The following is an explanation of the various columns found in Table B.2. The resulting data is used in the error analysis to determine the error bars as shown in Fig. (5.4), (5.5), and (5.6). Upper-case letters designate the columns.

A: Specification of the flowmeter employed for the current trial.

B: Value of the average specific gravity to which the density ball is adjusted.

C: Specific gravity below which the ball is predicted to sink (Eq. (2.3)).

D: Specific gravity at which the ball actually sank (Eq. (4.8)).

E: Total mass of ball (including liquid inside).

F: Flow rate for which the ball sinks below the surface was recorded. This is an average for seven separate trails.

G: Flow rate for which the ball sinks below the surface was recorded. This is the maximum of seven trials.

H: Flow rate for which the ball sinks below the surface was recorded. This is the minimum of seven trails.

J: Flow meter repeatability as given in Table B.1 at the average flowrate.

K: Flowmeter resolution as given in Table B.1 at the average flowrate.

L: Flow rate for which the ball sinks below the surface was recorded. This is the half of the difference between the maximum flow rate and the minimum flow rate $\frac{G-H}{2}$,

where G, and H are the results form columns G, and H respectively.

M: The uncertainty in measuring the flow rate at which the ball actually sank. $\sqrt{J^2+K^2+L^2}$,

where J, K, and H are the results form columns J, K, and L respectively.

N: The uncertainty in measuring the height when the bubbles are turned on and steady state has been reached. We assess this uncertainty to be $\pm 0.25\ mm$, independent of flowrate.

O: Flow rates ranging from 0 to 139 l/min, at 15 different values, were set at the nitrogen source, and the corresponding changes in height were recorded. A 3rd order polynomial was used in a least squares fit through the points

$$f(\Delta h) = -0.171507 + 0.419662(Q) + 3.330407\times10^{-4}(Q)^2 + 3.297877\times10^{-5}(Q)^3.$$

This was evaluated at the average flow rate $Q = Q_{avg}$

P: The change in $f(\Delta h)$ with respect to the change in the average flowrate Q_{avg}.

$$\frac{\partial f(\Delta h)}{\partial Q} = 9.89363E-5(Q)^2 + 6.66081E-4(Q) + 0.419662.$$

This was evaluated at the average flow rate $Q = Q_{avg}$

Q: The uncertainty in the change in height.

$$\delta(\Delta h) = \sqrt{(\delta h)^2 + (\partial f(\Delta h)/\partial Q)^2 (\delta Q)^2}.$$

R: The overall uncertainty of the fluid specific gravity.

$$\frac{\delta\rho}{\rho_w} = \frac{1}{(1 + \Delta h/h_o)^2}\frac{\delta(\Delta h)}{h_o}$$

A	B	C	D	E	F	G	H	J	K	L	M	N	O	P	Q	R
	Specific Gravity															
Flowmeter	Avg	Predicted	Actual	Mass	Flowrate			Flowmeter		Experiment						
Name	Ball	Fluid	Fluid	Ball	Q_{avg}	Q_{max}	Q_{min}	Repeatability	Resolution	Repeatability	$\delta(Q)$	$\delta(h)$	$f(\Delta h)$	$\frac{\partial f(\Delta h)}{\partial Q_{avg}}$	$\delta(\Delta h)$	$\frac{\delta\rho}{\rho_w}$
				(g)	(l/min)	(l/min)	(l/min)									
Flow Sensor	0.700	0.7593	0.7308	388.81	138.0	139	137	2.00	0.5	1.00	2.29	0.25	150.7549	2.3957	5.51	0.0071
	0.750	0.7995	0.7713	416.58	125.6	127	124	2.00	0.5	1.50	2.55	0.25	123.0766	2.0634	5.28	0.0076
	0.800	0.8396	0.8114	444.36	111.9	114	111	2.00	0.5	1.50	2.55	0.25	97.0934	1.7321	4.44	0.0070
	0.850	0.8797	0.8678	472.13	89.3	90	88	2.00	0.5	1.00	2.29	0.25	63.4269	1.2679	2.95	0.0053
	0.900	0.9198	0.9091	499.90	69.1	70	68	2.00	0.5	1.00	2.29	0.25	41.3386	0.9380	2.21	0.0044
	0.910	0.9278	0.9186	505.46	63.9	65	63	2.00	0.5	1.00	2.29	0.25	36.5724	0.8656	2.05	0.0042
	0.920	0.9358	0.9296	511.01	57.4	59	56	2.00	0.5	1.50	2.55	0.25	31.2737	0.7842	2.06	0.0043
	0.930	0.9438	0.9371	516.57	52.7	53	52	2.00	0.5	0.50	2.12	0.25	27.7070	0.7290	1.63	0.0034
	0.935	0.9479	0.9468	519.34	46.3	47	45	2.00	0.5	1.00	2.29	0.5	23.2681	0.6629	1.60	0.0034
	0.940	0.9519	0.9528	522.12	42.1	43	41	2.00	0.5	1.00	2.29	0.25	20.5741	0.6235	1.51	0.0033
44l/min	0.950	0.9599	0.9609	527.67	36.1	37	34.0	0.09	0.5	1.50	1.58	0.25	16.9884	0.5730	1.04	0.0023
	0.960	0.9679	0.9701	533.23	28.9	29.5	28.0	0.07	0.5	0.75	0.90	0.25	13.0090	0.5213	0.69	0.0016
	0.970	0.9759	0.9780	538.78	22.1	23	21.5	0.06	0.5	0.75	0.90	0.25	9.6079	0.4826	0.66	0.0015
	0.980	0.9840	0.9853	544.34	15.3	16	14.5	0.04	0.5	0.75	0.90	0.25	6.4390	0.4530	0.65	0.0015
16l/min	0.990	0.9920	0.9922	549.89	8.30	8.75	8.0	0.02	0.25	0.38	0.45	0.25	3.3628	0.4321	0.54	0.0013

Table B.2 Error analysis data results

LIST OF REFERENCES

Crocker, Malcolm J., 1998, *Handbook of Acoustics*, John Wiley & Sons, pp 70-71.

Haberman, W.L., and Morton, R.K., September 1953, "An Experimental Investigation of the Drag and Shape of Air Bubbles Rising in Various Liquids," Report 802, Navy Department, The David W. Taylor Model Basin, Washington 7, DC, pp. 17-32.

Kinsler, Lawrence E., and others, 2000, *Fundamentals of Acoustics*, 4th ed., John Wiley & Sons, pp. 238-240, 234.

Lide, David R., *Handbook of Chemistry & Physics*, 74th ed., 1994, CRC Press Inc., pp 8.18-34.

McIver, Richard D., 1982, "Role of Naturally Occurring Gas Hydrates in Sediment Transport," American Association of Petroleum Geologists, Bulletin, 66:789.

Private communication from Dr. Mike Stumborg, Naval Surface Warfare Center, Dahlgren, VA, Telephone (401) 841-4286.

Rowe, Mary M. and Gettrust, J. F., 1993, "Methane Hydrate Content of Blake Outer Ridge Sediments," New York Academy of Science International Conference on Natural Gas Hydrates.

Sadiku, Matthew N.O., 1995, *Elements of Electromagnetics*, 2nd ed., Oxford University Press Inc., pp. 251-253.

Wallis, Graham B., 1969, "One-dimensional Two Phase Flow," McGraw-Hill Inc., pp. 263-264, 27.

THIS PAGE INTENTIONALLY LEFT BLANK

INITIAL DISTRIBUTION LIST

1. Defense Technical Information Center 2
   8725 John J. Kingman Rd., STE 0944
   Ft. Belvoir, Virginia 22060-6218

2. Dudley Knox Library 2
   Naval Postgraduate School
   411 Dyer Rd.
   Monterey, California 93943-5101

3. Physics Department 2
   Naval Postgraduate School
   833 Dyer Road
   Monterey, CA 93943-5002

4. Professor Bruce Denardo, Code PH/Db 5
   Department of Physics
   Naval Postgraduate School
   Monterey, CA 93943-5002

5. Professor Ashok Gopinath, Code ME/Gk 1
   Department of Mechanical Engineering
   Naval Postgraduate School
   Monterey, CA 93943-5146

6. Engineering & Technology Curricular Office, Code 34 1
   411 Dyer Road
   Naval Postgraduate School
   Monterey, California 93943-5101

7. National Defence Headquarters 2
   Louis St Laurent Bldg
   555 Boulevard de La Carriere
   Hull, Quebec
   Canada K1A 0K2
   Attn: DMSS 6-2 LCdr L.B. Pringle